# Inverse Modeling in Magnetic Source Imaging: Comparison of MUSIC, SAM(g2), and sLORETA to Interictal Intracranial EEG

**Karin L. de Gooijer-van de Groep,[1,2] Frans S.S. Leijten,[1] Cyrille H. Ferrier,[1] and Geertjan J.M. Huiskamp[1]***

[1]*Department of Neurology and Clinical Neurophysiology, Rudolf Magnus Institute of Neuroscience, University Medical Centre Utrecht, Utrecht, The Netherlands*
[2]*MIRA Institute for Biomedical Technology and Technical Medicine, Twente University, Enschede, The Netherlands*

**Abstract:** Magnetoencephalography (MEG) is used in the presurgical work-up of patients with focal epilepsy. In particular, localization of MEG interictal spikes may guide or replace invasive electroencephalography monitoring that is required in difficult cases. From literature, it is not clear which MEG source localization method performs best in this clinical setting. Therefore, we applied three source localization methods to the same data from a large patient group for which a gold standard, interictal spikes as identified in electrocorticography (ECoG), was available. The methods used were multiple signal classification (MUSIC), Synthetic Aperture Magnetometry kurtosis [SAM(g2)], and standardized low-resolution electromagnetic tomography. MEG and ECoG data from 38 patients with refractory focal epilepsy were obtained. Results of the three source localization methods applied to the interictal MEG data were assigned to predefined anatomical regions. Interictal spikes as identified in ECoG were also assigned to these regions. Identified regions by each MEG method were compared to ECoG. Sensitivity and positive predictive value (PPV) of each MEG method were calculated. All three MEG methods showed a similar overall correlate with ECoG spikes, but the methods differ in which regions they detect. The choice of the inverse model thus has an unexpected influence on the results of magnetic source imaging. Combining inverse methods and seeking consensus can be used to improve specificity at the cost of some sensitivity. Combining MUSIC with SAM(g2) gives the best results (sensitivity = 38% and PPV = 82%). *Hum Brain Mapp* 00:000–000, 2012. 

**Key words:** interictal; magnetoencephalography; intracranial EEG monitoring; source localization; inverse modeling; irritative zone

## INTRODUCTION

Magnetoencephalography (MEG) is used in the presurgical work-up of patients with focal epilepsy. With MEG, interictal data can be recorded and mapped, which helps to localize the irritative zone: the area of cortical tissue that generates interictal spikes and encompasses the epileptogenic zone [Rosenow and Luders, 2001]. The gold standard for delineating these zones is chronic intracranial electroencephalography (EEG), with electrodes placed either into the brain (depth-EEG) or over the cortical surface (electrocorticography, ECoG). Chronic intracranial EEG,

*Correspondence to: Dr. Geertjan J.M. Huiskamp, Department of Neurology and Clinical Neurophysiology, hp F02.230, University Medical Centre Utrecht, PO Box 85500, 3508 GA Utrecht, The Netherlands. E-mail: g.j.m.huiskamp@umcutrecht.nl

Received for publication 22 November 2010; Revised 30 December 2011; Accepted 2 January 2012

DOI: 10.1002/hbm.22049

Published online in Wiley Online Library (wileyonlinelibrary.com).

however, is invasive, inconvenient, and costly. Interictal MEG may help to substitute ECoG in some cases or at least to guide placement of electrodes and minimize their number. In a recent study [Agirre-Arrizubieta et al., 2009], we compared interictal ECoG and interictal MEG to see how interictal MEG reflects interictal ECoG. We concluded that MEG source imaging reliably localizes interictal ECoG spikes. All MEG spikes were associated with an interictal ECoG spike. Fifty-six percent of all regions with interictal ECoG spikes were identified by interictal MEG. MEG is, however, not an all-comprehensive substitute. Its lack of sensitivity could be explained by the stochastics of spike occurrence and limited acquisition time, the radial orientation of spike sources or source depth—factors that cannot easily be influenced. However, the choice of the inverse model necessary for source imaging may also play a role. If so, better clinical results might be obtained using different models.

Different source localization models have given rise to different solutions to the inverse problem [Baillet et al., 2001; Grech et al., 2008; Michel et al., 2004]. They can be divided into three families [Leijten and Huiskamp, 2008]. Most clinical studies have used only the first family: classical single or multiple dipole modeling in which a current dipole source model is fitted to the EEG or MEG data. Parameters that have to be estimated are the dipole position and strength. The second and third families have been used much less. In the second family, a source is found by scanning all possible positions in the brain. These methods require assumptions about which part of the measured data is signal and which is background or noise. The third family consists of linear inverse methods in which the data are modeled with only the source strengths as parameters for a distributed set of dipoles at fixed, known locations. Assumptions about or constraints on source strength are required for these methods.

In this study, we will compare three source imaging packages with inverse methods of the last two families of inverse solutions, i.e., multiple signal classification (MUSIC) [Mosher et al., 1992], Synthetic Aperture Magnetometry kurtosis [SAM(g2)] [Kirsch et al., 2006; Robinson et al., 2002], and standardized low-resolution electromagnetic tomography (sLORETA) [Pascual-Marqui, 2002]. SAM(g2) transforms MEG data into a functional image of spike-like activity and provides source time courses in voxels exhibiting high excess kurtosis [Kirsch et al., 2006; Robinson et al., 2002]. sLORETA is a weighted minimum norm inverse solution for EEG or MEG. It is a nonadaptive spatial filter dependent on sensor configuration. MUSIC and SAM(g2) belong to the second group of inverse solutions and sLORETA to the third group.

SAM(g2) and sLORETA are spatial filters. They make an estimation of noise covariance where MUSIC assumes the noise to be white. MUSIC and SAM(g2) presume the source to be focal and of dipolar origin. They are sensitive only to the dipolar portion of the source activity. They cannot detect activity that has spread over a significant cortical area. Pitfalls can be expected with extended sources and when sources are strongly correlated. With sLORETA simultaneously active sources can be separated, but only if their fields are distinct enough and of similar strength. With low signal-to-noise ratio, sLORETA reconstructions may have some source location bias and give blurred results. sLORETA and MUSIC need preselection of spikes. SAM(g2) avoids the human subjectivity in detecting spikes [Baillet et al., 2001; Kobayashi et al., 2005; Mosher and Leahy, 1998; Robinson et al., 2002; Sekihara et al., 2005; Wagner et al., 2004].

In the clinical context mentioned above, it should be clear that the issue is not the millimeter accuracy of MEG localizations but rather the sensitivity and specificity of MEG when it comes to identifying sublobar regions that show interictal activity. The source of the epileptic activity is unknown and can be complex, which makes fine tuning of inverse methods for each particular patient difficult. More often ready-to-use software packages with a specific inverse method are used. From literature, it is not yet clear which source localization method performs best in this clinical setting. Simulation studies using EEG have suggested that in the analysis of real interictal spikes results from different methods should always be taken into account [Grova et al., 2006]. Therefore, we compared software packages with the often used MUSIC, SAM(g2), and sLORETA modeling in MEG source imaging of focal epilepsy, by applying the three methods to the same data from a large patient group for whom a gold standard of ECoG was available. This study gives more insight in the difference in results of methods used in clinical practice.

## MATERIALS AND METHODS

### Patients

Data were obtained from 38 patients with refractory focal epilepsy who underwent chronic intracranial EEG monitoring (subdural ECoG) and MEG registration as part of their presurgical work-up between 1998 and 2008. MEG results using the MUSIC inverse algorithm were available and used for implantation strategy. All patients were treated in the University Medical Centre in Utrecht as part of the national Collaborative Dutch Epilepsy Surgery Program. Approval for the MEG studies was given by the Medical Ethics Committee of the hospital.

### MRI

As part of a dedicated MRI epilepsy protocol, preoperative whole-head high-resolution 3D T1 sequences at 1.5 and 3 T (Philips Achieva, Best, The Netherlands) were available, allowing accurate segmentation of the cortical gray matter at a resolution of 1.5 mm.

### Chronic ECoG

Chronic ECoG was performed with subdural electrodes (Ad-Tech, Racine, WI) that were introduced through a

craniotomy, 80–120 electrodes per patient. Interelectrode distance was 1 cm. Data were acquired at a sampling rate of 400 or 512 Hz at a resolution of 12 or 16 bits. Appropriate antialiasing filters and a hardware high-pass filter of 0.16 Hz were used. ECoG was continuously recorded 24 h a day for an average of 7 (range: 3–10) days. In one patient, a single depth electrode was also placed, which was not used in the data comparison. The electrodes were localized by comparing digital photographs during and after implantation and by a postimplantation CT scan that was matched to a MRI volume acquired preoperatively [Noordmans et al., 2001]. The electrode positions from various viewpoints were projected on the preimplantation MRI cortex rendering.

## MEG

MEG recordings were obtained in a 151-channel whole-head MEG system (Omega 151; CTF Systems, Port Coquitlam, British Columbia, Canada) at the MEG Centre of the Free University Medical Centre in Amsterdam. The MEG system consisted of axial gradiometers distributed in a helmet-shaped array inside a Dewar filled with liquid helium. Spontaneous activity was recorded at a sample rate of 625 or 1,250 Hz with a 32-bit resolution. Antialiasing filters were used (208 or 416 Hz). At least 60 min of MEG data was obtained from each patient. Head position was measured before and after each session of around 10 min. Head-shape information was acquired by marking up to 100 anatomic landmarks on the skull using a fourth coil for more accurate MRI coregistration [de Munck et al., 2001].

## MEG Spike Identification for MUSIC and sLORETA

Two clinical neurophysiologist independently marked interictal transients in MEG datasets. High- and low-pass filters were set at 0.7 and 70 Hz, respectively. A total of 60–90 min of interictal MEG data was analyzed for each patient. Kappa statistics were calculated between the interictal epileptiform transients marked by the two independent observers for each MEG recording. Only MEG recordings for which there was sufficient agreement (inter-observer kappa $> 0.4$) were accepted. For these, consensus interictal epileptiform transients were then defined as interictal epileptiform spikes. An automated clustering algorithm [van 't Ent et al., 2003] was performed to segregate different interictal epileptiform spikes. In this algorithm, MEG data centered on selected spikes were normalized, and Euclidean distances between spike representations were input to a Ward's hierarchical clustering algorithm. With this method, a reliable categorization of epileptiform spikes can be obtained. The spikes from each cluster were averaged and tested for homogeneity by plotting the averaged spikes and their standard deviations. When the standard deviation of the cluster was larger than one-third of the spike maximum, the cluster was rejected. Clusters of spikes that were part of physiological rhythms were discarded.

## MEG Spike Modeling: sLORETA and MUSIC

The averaged clusters of spikes were modeled using Curry 3.0 software (Philips Medical Systems, Hamburg, Germany) for MUSIC and NUTMEG 1.0 [Dalal et al., 2004] for sLORETA. For both methods, a single-shell spherical head model was used as forward model. MRI anatomical landmarks were matched to those recorded during the MEG session. MUSIC resolution was 3 mm and sLORETA was 5 mm. For both methods, the region of interest was the whole brain. The interval from the beginning of the rising slope of the spike to the spike maximum was used for MUSIC analysis [Leijten and Huiskamp, 2008]. Principal component analysis determined the separation between noise and signal subspace. Locations for which the resulting MUSIC metric exceeded two-thirds of the overall maximum were displayed on a cortical rendering from MRI. The same clusters of spikes were also used for sLORETA analysis. For sLORETA an additional high-pass filter of 1 Hz was applied. Also, data were selected such that it had the peak of interest in it but also a large enough time window around this peak to further ensure that the sensor covariance matrix was not too singular (mean length = 141 ms and standard deviation = 23 ms). For regularization, Tikhonov regularization was used. A fixed regularization parameter was used, which was set at the safe side, avoiding spurious results. The time around the spike maximum showing the highest estimated local current density was used. A threshold was set at 90% of the current density and voxels exceeding this threshold were displayed in a 3D MRI.

## SAM(g2)

The SAM(g2) analysis [Kirsch et al., 2006; Robinson et al., 2002] was performed using software tools provided by VSM MedTech/CTF Systems (Port Coquitlam, British Columbia, Canada). In SAM, a scalar beamformer is used that is obtained by optimizing the source moment vector direction from the data. Multiple local spheres were used as forward model. To eliminate the background activity and contrast the interictal spike activity, SAM(g2) analysis was performed with a bandpass filter of 20–70/200 Hz. A total of 20–70 Hz is used in several studies [Ishii et al., 2008; Kirsch et al., 2006] and is outside the range of alpha-band activity that would tend to drive the excess kurtosis negative. SAM(g2) was performed on raw datasets with lengths between 100 and 900 s without visible artifacts. In some patients two datasets were used. Segments with muscle artifacts were avoided. MEG data were transformed in virtual sensor waveforms for every voxel in the region of interest,

which was again the whole brain, at steps of 5 mm. For each coordinate in the head, the excess kurtosis (g2) was computed for its virtual sensor waveform. Excess kurtosis is a measure of the statistical distribution of sample amplitudes and is independent of absolute amplitude or the order in which samples are selected. Excess kurtosis was computed from each source waveform as $g_2 = \frac{1}{K\sigma^4}\sum_{k=1}^{K}[S_k - S]^4 - 3$, where $k$ is the sample index, $K$ is the total number of samples, and $\sigma$ is the standard deviation of the time series $S(k)$. The excess kurtosis is unitless. The presence of spikes implies statistical outliers from a normal distribution function. Normal brain source activity can have a small positive kurtosis of $<0.5$.

An image was made up of the $g_2$ values corresponding to each voxel. The threshold to detect peaks in the volumetric image and the peak-to-root mean square ratio to detect spikes in the virtual sensors were set to 1.0 and 6.0, respectively. Virtual sensors and the marked spikes were used to recognize muscle activity and other artifacts. Sets that still contained muscle activity or artifacts were reanalyzed without the trials containing these artifacts. The final virtual sensors that showed excess kurtosis of half the maximum (but higher than 1.0) were displayed on the 3D MRI. For SAM(g2), the maximum of the virtual sensor was localized and its surrounding area that had kurtosis of about half the maximum.

## ECoG Spikes

For each patient, two clinical neurophysiologists selected up to 60 min of representative samples of awake interictal ECoG spikes. These samples included all different interictal ECoG spikes observed during the recording period. These representative interictal ECoG data were analyzed by consensus. Data were rereferenced to an indifferent intracranial electrode for review. High- and low-pass filters were set to 0.53 and 70 Hz, respectively. The different spikes were identified and averaged in the interictal ECoG data set. For scalp and intracranial EEG, the relevance of taking synchronous surface area into consideration has been emphasized by several authors [Alarcon et al., 1994; Mikuni et al., 1997; Oishi et al., 2002; Shigeto et al., 2002; Tao et al., 2005, 2007]. This is because compound EEG/MEG activity can be considered as the sum of multiple potential fields generated in a synchronously activated surface area. For ECoG no accurate source model is available for this yet. Therefore, we used the method described by Agirre-Arrizubieta et al. [2009]: for each averaged ECoG spike, a combined amplitude and synchronous surface-area measure was calculated to characterize the data. Spikes were related to the background. The comparison with the background for each electrode indicated whether the spatial extent of the averaged spike could be estimated reliably. Only spikes where at least one of the electrodes met the background criteria were plotted on the CT-MRI rendering by marking each electrode that met these criteria.

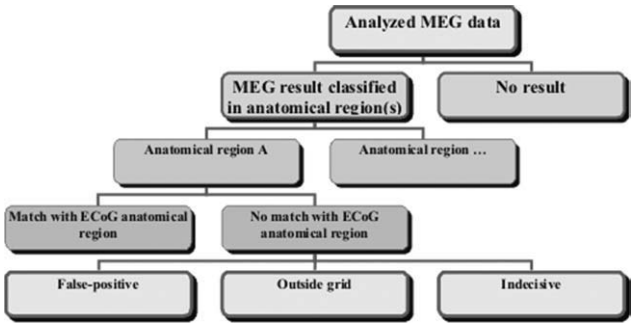


**Figure 1.**
Classification of MEG results. An MEG result is accorded to predefined anatomical region(s) (single or multiple). For anatomical region A, the possible comparison categories with ECoG are shown. This is repeated for all regions covering the cortex.

## Brain Anatomical Regions

Anatomical landmarks such as central sulcus and the Sylvian fissure and the electrocortical stimulation function mapping results were used, in the neurosurgical sense, to define specific anatomical cortical brain regions, as described in the article by Agirre-Arrizubieta et al. [2009]. These regions are the central, parietal, and occipital lobes. The frontal lobe was divided in the frontal superior, medial, inferior, and fronto-orbital regions; the temporal lobe into the lateral and mesial regions, the latter comprising the amygdale, the hippocampus, the parahippocampal gyrus, and the temporal-basal area. The interhemispheric region, finally, consisted of the mesial surface of the frontal, parietal, and occipital lobes.

## Association Method and Interpretation of the Results

Two specialists, independently, in random order and blinded for patient name, allocated the results of MEG source imaging using MUSIC, SAM(g2), and sLORETA and each interictal ECoG spike to its predefined anatomical region(s). In case of discrepancy, consensus was sought. Anatomical regions found by each MEG method were compared to the ECoG. MEG results were classified as "match," "indecisive" or "false positive" (Fig. 1). When there was overlap within the same anatomical region between ECoG and MEG, we called this a "match." When MEG results were outside the area covered by electrode grids, outside the brain cortex, or were localized over a very large area, this was an "indecisive" result. "False positives" were MEG results in a region covered by grids, but having no ECoG counterpart (Fig. 2A). A false positive could be partial, as shown in Figure 2B where an MEG result localizes in the lateral temporal and in the central lobe (the precentral and postcentral gyrus). There is, however, only a corresponding ECoG result in the temporal

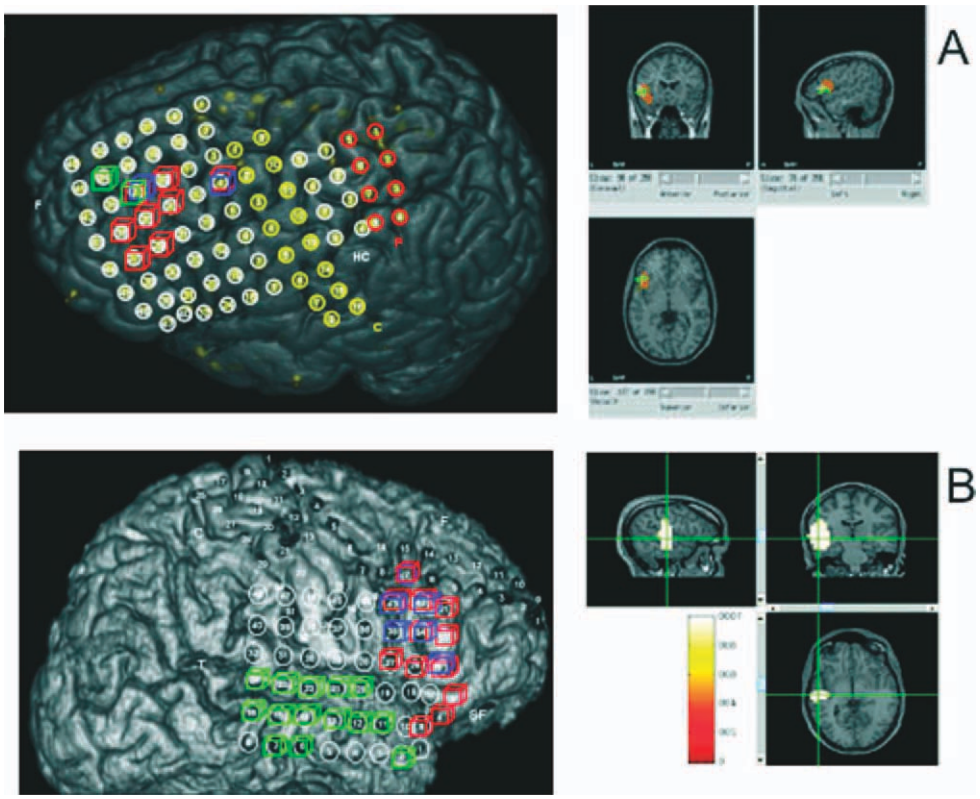


**Figure 2.**

Two examples of false-positive results. On the left: cubes in different colors represent different ECoG spikes found. **A**: The SAM(g2) result (right) is in the frontal inferior region, where there is grid coverage but no match (left). **B**: The sLORETA result (right) overlaps in the lateral temporal region, but the part in the central region has no ECoG match.

region. Although partially correct in the temporal lobe, we classified the central part as "false positive." Note that this approach is more stringent than in our early study [Agirre-Arrizubieta et al., 2009]. After comparing individual results in this way, the sensitivity and positive predictive value (PPV) of each MEG inverse method were calculated overall and for each anatomical region using, respectively, the following formulas:

$$\text{sensitivity}(\%) = \frac{\text{Number of true positives}}{\text{Number of true positives} + \text{number of false negatives}} \times 100$$

$$\text{PPV}\ (\%) = \frac{\text{Number of true positives}}{\text{Number of true positives} + \text{number of false positives}} \times 100$$

## RESULTS

Four of the 38 patients were excluded because their ECoG datasets did not contain at least 60 min of representative recordings or because of excessive artifacts in the MEG data.

### Spikes

For MUSIC and sLORETA, MEG spikes were scored by two human observers. In 30 of the 34 patients (88%), the agreement was sufficient (kappa $> 0.4$) to allow spike modeling. MUSIC and sLORETA were then applied to 53

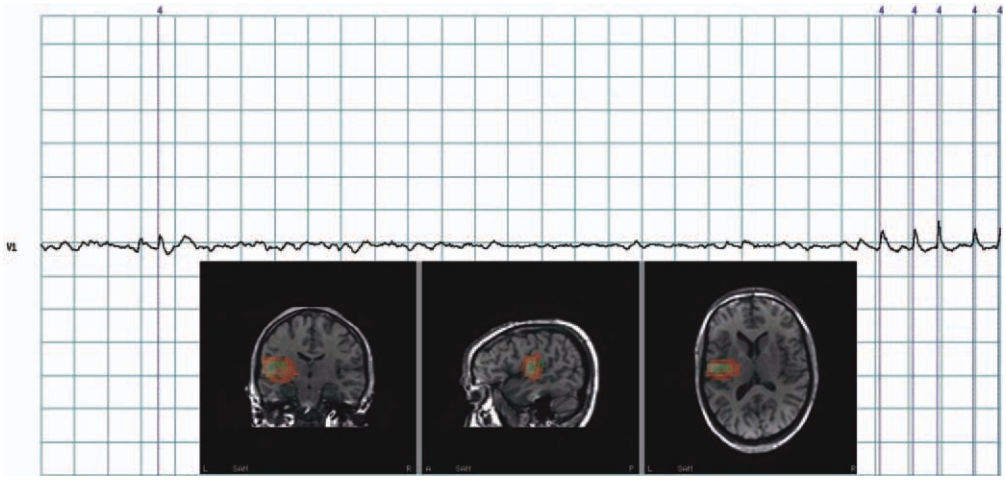

**Figure 3.**
Virtual sensor, SAM(g2) automated detections (green lines) and SAM(g2) source imaging result in a patient.

averaged clusters of spikes in these 30 patients. sLORETA gave one result located outside the cortex, which was marked as indecisive.

For SAM(g2) all 34 patients were analyzed, as the method does not depend on the presence of visually identified spikes. In three patients (9%), the kurtosis threshold of 1.0 was not reached and results were considered negative. These were different patients from the three patients with a low kappa value mentioned above. A depiction of a virtual sensor in MRI space is given in Figure 3. Nine patients gave indecisive results.

Representative interictal ECoG of 34 patients was analyzed. After identification, averaging, and characterization, 238 different spikes were plotted on the CT-MRI rendering with ECoG electrode positions (e.g. see Fig. 2, left part). Of the 238 interictal ECoG spikes, 50% showed a MUSIC correlate, 46% a SAM(g2) correlate, and 47% a sLORETA correlate. Combination of two or three methods gave a better overall match with ECoG. All three source imaging models together captured the regions of 70% of the interictal ECoG spikes.

## Anatomical Regions

The 238 ECoG spikes represented 154 anatomical regions, i.e., some ECoG spike clusters in one patient were within the same region. MUSIC found 39 (25%), SAM(g2) 37 (24%), and sLORETA 41 (27%) of these regions. Again, combining two or three methods gave a higher association between ECoG and MEG. MUSIC, SAM(g2), and sLORETA together gave the best result with 75 regions (49%) identified (Fig. 4A).

Only one patient showed a MUSIC results outside the intracranial electrode grid covering. This was 7 for SAM(g2) and 3 for sLORETA.

### *False positives*

All methods gave false positives (Fig. 4B,D), but most were partial false positives. This was often the case when an MEG result was found around the Sylvian fissure (see Fig. 2B) or in the frontal lobe. sLORETA gave the largest number of false positives. Even when there was agreement between two or three methods, some false positives remained (Fig. 4D).

### *Comparing MEG inverse methods*

Matching any two methods, and taking the agreement between the two as a criterion, gave fewer identified regions than all three taken together. MUSIC and sLORETA gave the highest match. Ten regions in seven patients were identified that were concordant between all three methods (Fig. 4C); this was almost always (7/10) the lateral temporal region. In three patients, all MEG results were negative in areas covered by grids. Two of them had a MEG set with low interobserver kappa. In one patient with a low kappa data set (therefore excluded from MUSIC and sLORETA analysis), SAM(g2) did find a positive result. sLORETA was the only method with a match with ECoG in one patient. For MUSIC this was the case in three patients (all three showing low kurtosis values of $<1.0$).

### *Results per anatomical region*

Table II gives total and regional sensitivity and PPV of each MEG inverse methods. The occipital region was left out of the sensitivity table, because there was only one ECoG result.

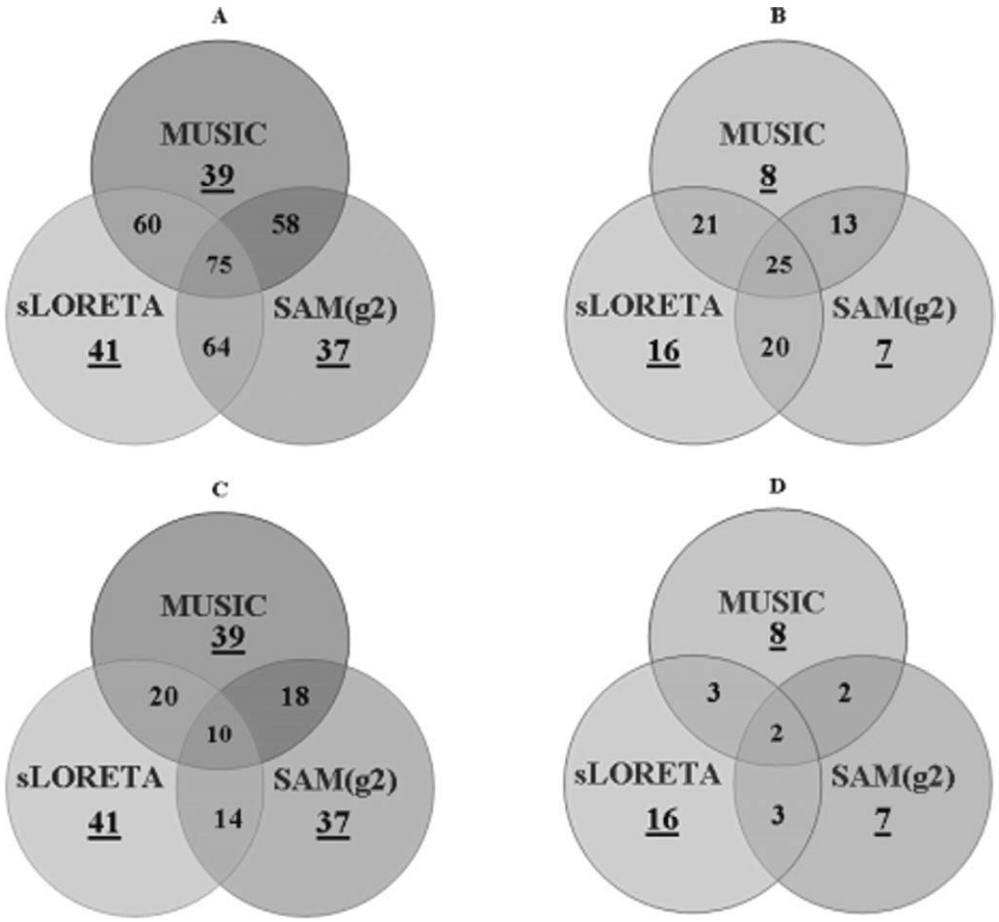


**Figure 4.**
**A**: Cumulative number of ECoG regions found with one, two, or three MEG inverse methods. **B**: Cumulative number of false positives found using one, two, or three MEG methods. **C**: Number of ECoG regions found using one MEG method (underlined) and concordances (overlap). **D**: Number of false positives found using one MEG method (underlined) and concordances (overlap).

## DISCUSSION

### Clinical Conclusions

At first sight, the sensitivity of MEG source imaging methods looks similar (Table II). In fact, if the three methods would have been evaluated independently on the basis of the same data, the conclusion would have been that their performance is similar, and no recommendation for a particular method would have been given. However, the methods do differ in what they detect. Thus, the choice of inverse models has a remarkable influence on the yield of magnetic source imaging. As can be seen from the table, the number of detected regions with spikes in the ECoG doubles from around 25% using any inverse model alone (Table II) to almost 50% when results from all three models are combined (Table III). This comes at a cost of an

**TABLE I. Positive predictive value for each single method, combination of methods, and concordance of methods**

| Positive predictive value | MUSIC | SAM(g2) | sLORETA | MUSIC + SAM(g2) | MUSIC + sLORETA | SAM(g2) + sLORETA | MUSIC + SAM(g2) + sLORETA |
|---|---|---|---|---|---|---|---|
| Single methods | 83% | 84% | 72% | — | — | — | — |
| Combination of methods | — | — | — | 82% | 74% | 76% | 75% |
| Concordance of methods | — | — | — | 90% | 87% | 82% | 83% |

**TABLE II. Sensitivity and false-positive results of the MEG source imaging methods alone for each anatomical region and overall**

| | | MUSIC | | SAM(g2) | | sLORETA | |
|---|---|---|---|---|---|---|---|
| | ECoG spike regions | Match with ECoG | False positives | Match with ECoG | False positives | Match with ECoG | False positives |
| Frontal | 60 | 3 (5%) | 2 (3%) | 13 (22%) | 6 (10%) | 12 (20%) | 8 (13%) |
| Temporal | 47 | 18 (38%) | 0 (0%) | 13 (28%) | 0 (0%) | 9 (19%) | 1 (2%) |
| Central | 17 | 4 (24%) | 3 (18%) | 4 (24%) | 1 (6%) | 8 (47%) | 5 (29%) |
| Parietal | 16 | 4 (25%) | 2 (13%) | 5 (31%) | 0 (0%) | 5 (31%) | 2 (13%) |
| Interhemispherical | 13 | 9 (69%) | 1 (8%) | 1 (8%) | 0 (0%) | 6 (46%) | 0 (0%) |
| (Occipital) | (1) | (1) | (0) | (1) | (0) | (1) | (0) |
| Overall | 154 | 39 (25%) | 8 (5%) | 37 (24%) | 7 (5%) | 41 (27%) | 16 (10%) |

equal doubling in false-positive MEG results from 5–10% to 16%. Most of the false positives are due to sLORETA. Running MUSIC and SAM(g2) algorithms on the same MEG data improves the identification of spike regions in the ECoG by almost 15% with only a small increase of 3% in false positives (Table III). This may help to guide electrode placement in patients planned for intracranial EEG, as such an approach upholds the high reliability of MEG source imaging while improving its relatively low sensitivity, based on the very same MEG data.

Combining inverse methods and seeking consensus can also be used to further improve specificity of the results to almost 100% (Table I). Unfortunately, if overlap between methods is thus used, the number of results drops substantially. Again, sLORETA seems least helpful. Concordance between MUSIC and SAM(g2) gives the maximum specificity with at least some sensitivity left. All three methods are most consistent in localizing sources in the temporal lobe (Table IV). Least regions are found in the frontal lobe. MUSIC and sLORETA are better in localizing in the interhemispheric region compared with SAM(g2).

Before we will come to a practical advice, we will try to answer the question why these inverse methods may have such a surprising complementariness and discuss some of the limitations of our study.

## Reasons for Complementariness

MUSIC and sLORETA were applied to the same, visually scored MEG spikes. Our expectation, therefore, was that exactly the same anatomical regions would be found in the majority of cases. However, this was actually the case in only three patients. The explanation could be that most spikes are complex and originate from different anatomical regions, a situation for which each method has a different sensitivity, or that bias occurred in one or either method. Relative bias in MUSIC and SAM compared with sLORETA can be expected in sources that are highly correlated. Another bias of MUSIC and SAM is the constraint that a source should be dipolar. Methods also perform differently when not both the maximum and minimum of the MEG field are covered by the MEG helmet. Figure 5 shows the effect of a source in the tip of the temporal lobe. Only when the head is surrounded completely by a MEG helmet, the whole magnetic field would be detected. In this example, the assumption of dipolarity of MUSIC and SAM may work out differently in the resulting solution than for the distributed model underlying sLORETA. Model simulations done by our group confirmed this (unpublished results).

Because we are dealing with nonsimultaneous data, not all bias and attendant wrong localization will end up as a

**TABLE III. Sensitivity and false-positive results of the MEG source imaging methods in combination for each anatomical region and overall**

| | | MUSIC + SAM(g2) | | MUSIC + sLORETA | | SAM(g2) + sLORETA | | MUSIC + SAM(g2) + sLORETA | |
|---|---|---|---|---|---|---|---|---|---|
| | ECoG spike regions | Match with ECoG | False positives | Match with ECoG | False positives | Match with ECoG | False positives | Match with ECoG | False positives |
| Frontal | 60 | 15 | 7 | 14 | 9 | 23 | 12 | 24 | 13 |
| Temporal | 47 | 19 | 0 | 19 | 1 | 15 | 1 | 20 | 1 |
| Central | 17 | 6 | 3 | 10 | 6 | 10 | 5 | 11 | 6 |
| Parietal | 16 | 8 | 2 | 6 | 4 | 8 | 2 | 9 | 4 |
| Interhemispherical | 13 | 9 | 1 | 10 | 1 | 7 | 0 | 10 | 1 |
| (Occipital) | (1) | (1) | (0) | (1) | (0) | (1) | (0) | (1) | (0) |
| Overall | 154 | 58 (38%) | 13 (8%) | 60 (39%) | 21 (14%) | 64 (42%) | 20 (13%) | 75 (49%) | 25 (16%) |

**TABLE IV. Sensitivity and false-positive results of the MEG source imaging methods using only concordant results for each anatomical region and overall**

| | | MUSIC + SAM(g2) | | MUSIC + sLORETA | | SAM(g2) + sLORETA | | MUSIC + SAM(g2) + sLORETA | |
|---|---|---|---|---|---|---|---|---|---|
| | ECoG spike regions | Match with ECoG | False positives | Match with ECoG | False positives | Match with ECoG | False positives | Match with ECoG | False positives |
| Frontal | 60 | 1 | 1 | 1 | 1 | 2 | 2 | 0 | 1 |
| Temporal | 47 | 12 | 0 | 8 | 0 | 7 | 0 | 7 | 0 |
| Central | 17 | 2 | 1 | 2 | 2 | 2 | 1 | 1 | 1 |
| Parietal | 16 | 1 | 0 | 3 | 0 | 2 | 0 | 1 | 0 |
| Interhemispherical | 13 | 1 | 0 | 5 | 0 | 0 | 0 | 0 | 0 |
| (Occipital) | (1) | (1) | (0) | (1) | (0) | (1) | (0) | (1) | (0) |
| Overall | 154 | 18 (12%) | 2 (1%) | 20 (13%) | 3 (2%) | 14 (9%) | 3 (2%) | 10 (6%) | 2 (1%) |

false-positive result. A wrongly modeled result may still coincide with another ECoG spike localization. Figure 6 shows the cluster and its dipole field that MUSIC localized purely in the temporal lobe and sLORETA more centroparietally. This patient did show central and parietal interictal ECoG activity, but the question is whether sLORETA localized this or actually mislocalized the temporal spike. The low amplitude of the negative flux in channel MLT35 compared with the large flux in MLT22 and the fact that there is negative flux contralaterally supports the assumption that the MEG helmet did not cover the negative maximum. In the same patient, source imaging of somatosensory evoked field data, where the whole magnetic dipole field is covered by the MEG helmet, showed no difference between MUSIC and sLORETA results.

Blurred results can occur due to the regularization that is required in sLORETA. This could also be an explanation for different results between MUSIC and sLORETA. We used a fixed regularization parameter, set at the safe side, so with a bias toward more smooth results. We did check, in a number of cases, a data-dependent parameter, but results did not differ much. More importantly, a high threshold was used for sLORETA, but even then most sLORETA results cover more than one contiguous anatomical region, probably resulting in a high number of (partial) false positives. Some sLORETA results projected over both sides of the Sylvian fissure and had to be allocated to both the lateral temporal and the central regions. In clinical terms, this ambiguity is definitively unwanted, as these areas require a very different surgical approach and have a different surgical prognosis. Other false positives were found in the central and frontal lobes. This could be an artifact of our classification method because the predefined frontal regions are close to each other, just as the relatively small central region is neighboring various other brain regions.

Simultaneously active sources can be seperated by sLORETA, but only if their fields are distinct enough and

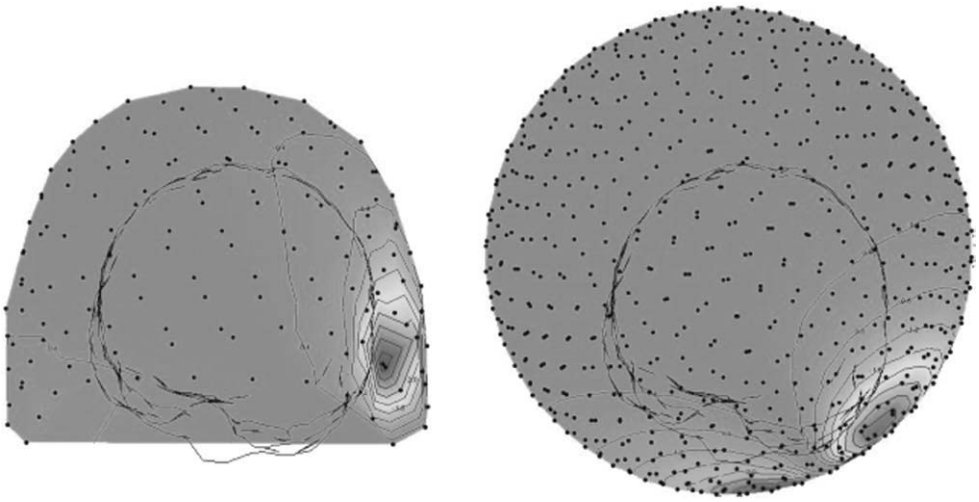

**Figure 5.**
Dipole field detected in the real MEG helmet (left) and in an imaginary sphere surrounding the whole head (right).

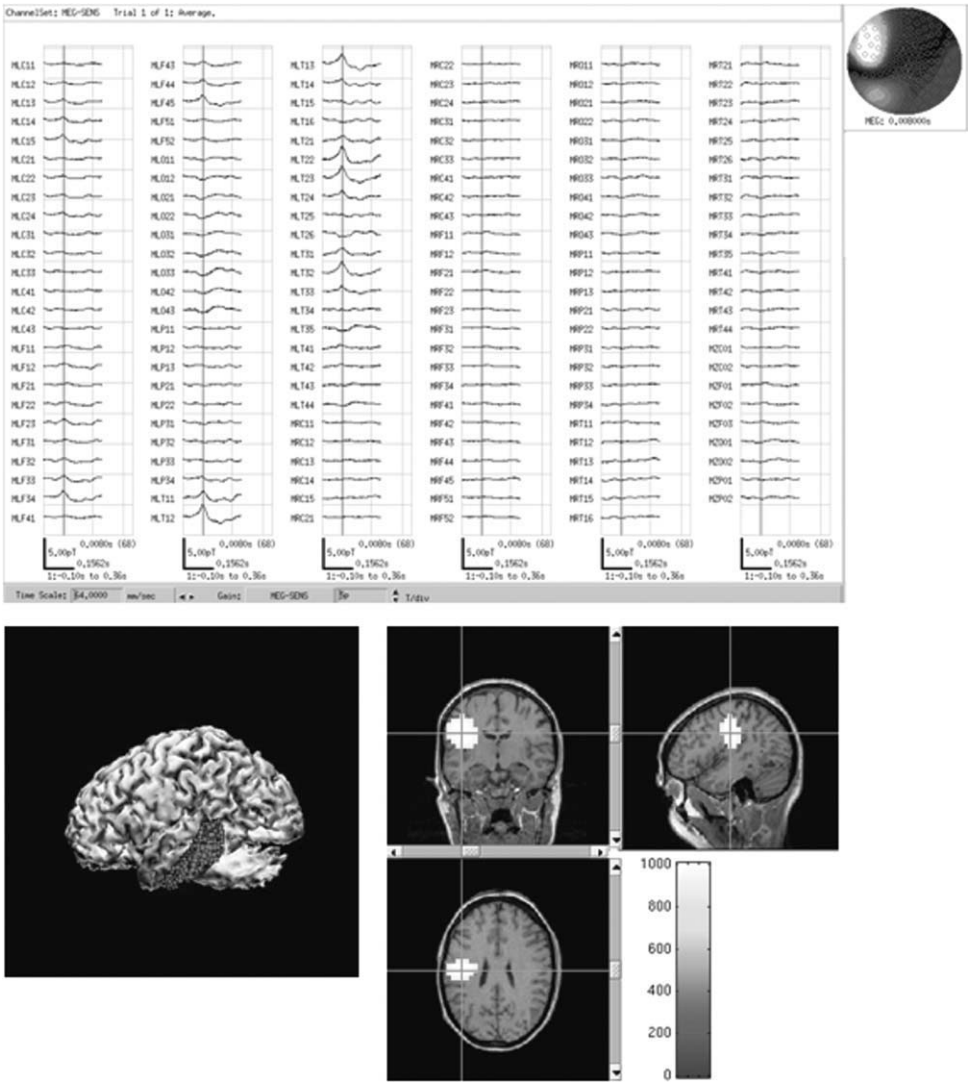


**Figure 6.**
Averaged spike cluster (top left) with corresponding dipole field (top right) and source imaging results using MUSIC on a rendered brain (bottom left) and sLORETA (bottom right).

of similar strength. In the context of a strong or superficial source, week or deep sources remain invisible and nearby sources of similar orientation tend not to be separated but interpreted as one source located in between [Sekihara et al., 2005; Wagner et al., 2004].

Spikes for MUSIC and sLORETA analysis were marked visually. This might give a bias toward superficial sources, ignoring the interictal spikes that are difficult to detect in MEG, which can originate from deep source. As a consequence, results by MUSIC and sLORETA that are deep are likely false localizations. In the mesial temporal region, e.g., many high amplitudes were seen in the ECoG in our patient population, but few results were found there by MEG. Because ECoG and MEG were not recorded simultaneously, it remains difficult to establish which interictal spikes seen in ECoG are invisible in MEG. In general, source location, orientation, extent, and curvature can explain the sensitivity of MEG for interictal spikes [Huiskamp et al., 2010].

SAM(g2) uses the "spikiness" of the data, i.e., it favors estimated source waveforms with a high kurtosis value. Instances of high "spikiness" in the virtual sensors, however, do not always equal what human observers see as spikes. This makes SAM(g2) from the outset a truly independent method from the other two. Sometimes not even a single spike of the human observers was found by SAM(g2), or markers were placed where nothing was identified by visual inspection. Of course, this could be

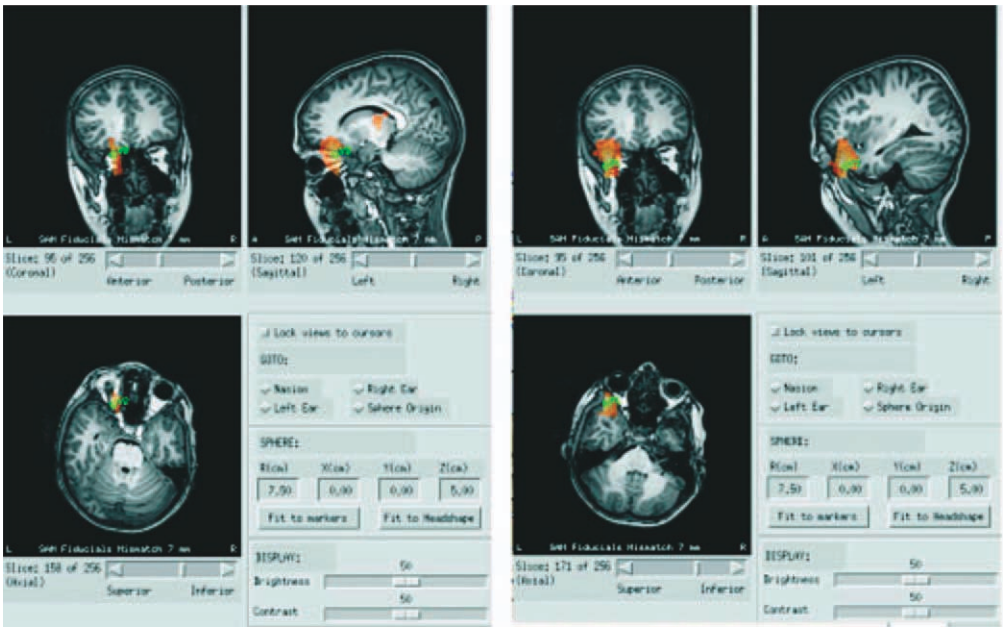

**Figure 7.**
SAM(g2) results for the same dataset using different high-pass filters. Left: high-pass filter of 20 Hz (first virtual sensor in ventricle); right: high-pass filter of 10 Hz.

due to SAM(g2)'s optimal spatial filter for the virtual sensors. The virtual signal in this sensor may reveal spikes hidden in the MEG signal itself. SAM(g2) would thus seem especially attractive when the MEG data show no or sparse spikes. Indeed, SAM(g2) gave good results in one such patient (four of five ECoG regions found). Interestingly, no results were found in the hippocampus. Yet, more research is necessary. Optimal settings are not well established. In some patients, we tried a high-pass filter different from the suggested 20 Hz, leading to results with higher kurtosis and better concordance with ECoG data. In other patients, this had no effect or an adverse effect. Figure 7 shows the results in one patient. Using a high-pass filter of 20 Hz, two not very clear results were found (one source outside the brain) with a kurtosis value around 1.0. The region found was frontal. Setting the high-pass filter at 10 Hz, the kurtosis value was much higher (8.4) and a clear region was identified, which was temporal. The ECoG showed that only the latter result was true. Similar effects for different low-pass filter setting may be expected.

## LIMITATIONS

Although interictal ECoG is the gold standard for interictal MEG, a disadvantage is its limited coverage of the brain. Especially, SAM(g2) gave a lot of results outside the area covered by grids (seven patients). There is a bias in the placement of the grids, as MEG MUSIC results were available before electrode placement. As a result, fewer source localizations outside the grids were to be expected using MUSIC. sLORETA, based on the same spikes as MUSIC, found fewer results outside the grids than SAM(g2). As a consequence of our approach to use ready-to-use software packages different forward models were used: multiple spheres for SAM(g2) and a single sphere for sLORETA and MUSIC. It has been shown that the effect of this on localization of interictal spikes for MEG is negligible, even when using realistic models [Scheler et al., 2007]. Volume conductor effects can influence estimated dipole orientation [Huiskamp, 2004]. This can have an influence when orientation is used as a constraint, which is not the case in our study.

## RECOMMENDATIONS

In difficult cases for epilepsy surgery, especially when intracranial investigations seem warranted, MEG is a worthwhile noninvasive study. Interictal MEG source imaging results are extremely reliable using sophisticated inverse models, in that MEG will localize areas with interictal spikes in the ECoG. Thus, when available, MEG results should always be taken into account in placing electrode grids. Unfortunately, MEG results reveal only a minority of interictally active regions and, therefore, do not substitute the ECoG. Surprisingly, without the need for ancillary MEG recordings, the relatively low sensitivity of MEG can be improved by combining different inverse source models. We, therefore, advise to incorporate two such models, MUSIC and SAM(g2), into the routine of

presurgical magnetic source imaging. Both methods can be seen as complementary.

### Future Directions

Subsequent research may take many forms. The performance of other advanced source localization methods must be tested (e.g., R-MUSIC [Mosher and Leahy, 1998], which deals with some disadvantages of MUSIC). Preprocessing algorithms may be developed to assist in choosing an inverse method for a particular dataset instead of our proposed combining. However, optimizing combined methods by using model averaging can be considered [Trujillo-Barreto et al., 2004]. More research has to be done on the optimal filter settings for SAM(g2). Virtual sensors of SAM(g2) data have to be studied thoroughly and compared to amplitude distributions in corresponding ECoG electrodes or kurtosis of source amplitude distributions as derived from sLORETA. A big challenge will be to deal with the effect of noise on the size of the MEG result. MEG results can be compared to EEG-fMRI findings, and these may also complement each other. Finally, it should be investigated if interictal MEG has a bias toward regions of ictal onset. If so, its relatively low sensitivity may even be a selective advantage. A reason to believe that this might be so is the fact that probably the regions with the largest synchronous surface area produce visible spikes. These may be the property that predisposes toward ictal epileptogenicity.

## ACKNOWLEDGMENTS

The authors thank the MEG Centre of the Free University Medical Centre in Amsterdam, The Netherlands, for their support and Epilepsy Centre Kempenhaeghe, Heeze, The Netherlands, for sharing MEG data.

## REFERENCES

Agirre-Arrizubieta Z, Huiskamp GJ, Ferrier CH, van Huffelen AC, Leijten FS (2009): Interictal magnetoencephalography and the irritative zone in the electrocorticogram. Brain 132:3060–3071.

Alarcon G, Guy CN, Binnie CD, Walker SR, Elwes RD, Polkey CE (1994): Intracerebral propagation of interictal activity in partial epilepsy: Implications for source localisation. J Neurol Neurosurg Psychiatry 57:435–449.

Baillet S, Mosher JC, Leahy RM (2001): Electromagnetic brain mapping. IEEE Signal Process Mag 18:14–30.

Dalal SS, Zumer JM, Agrawal V, Hild KE, Sekihara K, Nagarajan SS (2004): NUTMEG: A neuromagnetic source reconstruction toolbox. Neurol Clin Neurophysiol 2004:52.

Dalal SS, Zumer JM, Guggisberg AG, Trumpis M, Wong DD, Sekihara K, Nagarajan SS (2011): MEG/EEG source reconstruction, statistical evaluation, and visualization with NUTMEG. Comput Intell Neurosci 2011:758973.

de Munck JC, Verbunt JP, van 't Ent D, van Dijk BW (2001): The use of an MEG device as 3D digitizer and motion monitoring system. Phys Med Biol 46:2041–2052.

Grech R, Cassar T, Muscat J, Camilleri KP, Fabri SG, Zervakis M, Xanthopoulos P, Sakkalis V, Vanrumste B (2008): Review on solving the inverse problem in EEG source analysis. J Neuroeng Rehabil 5:25.

Grova C, Daunizeau J, Lina JM, Benar CG, Benali H, Gotman J (2006): Evaluation of EEG localization methods using realistic simulations of interictal spikes. Neuroimage 29:734–753.

Huiskamp G (2004): EEG-MEG source characterization in post surgical epilepsy: The influence of large cerebrospinal fluid compartments. Conf Proc IEEE Eng Med Biol Soc 6:4401–4404.

Huiskamp G, Agirre-Arrizubieta Z, Leijten F (2010): Regional differences in the sensitivity of MEG for interictal spikes in epilepsy. Brain Topogr 23:159–164.

Ishii R, Canuet L, Ochi A, Xiang J, Imai K, Chan D, Iwase M, Takeda M, Snead OC III, Otsubo H (2008): Spatially filtered magnetoencephalography compared with electrocorticography to identify intrinsically epileptogenic focal cortical dysplasia. Epilepsy Res 81:228–232.

Kirsch HE, Robinson SE, Mantle M, Nagarajan S (2006): Automated localization of magnetoencephalographic interictal spikes by adaptive spatial filtering. Clin Neurophysiol 117:2264–2271.

Kobayashi K, Yoshinaga H, Ohtsuka Y, Gotman J (2005): Dipole modeling of epileptic spikes can be accurate or misleading. Epilepsia 46:397–408.

Leijten FS, Huiskamp G (2008): Interictal electromagnetic source imaging in focal epilepsy: Practices, results and recommendations. Curr Opin Neurol 21:437–445.

Michel CM, Murray MM, Lantz G, Gonzalez S, Spinelli L, Grave de Peralta R (2004): EEG source imaging. Clin Neurophysiol 115:2195–2222.

Mikuni N, Nagamine T, Ikeda A, Terada K, Taki W, Kimura J, Kikuchi H, Shibasaki H (1997): Simultaneous recording of epileptiform discharges by MEG and subdural electrodes in temporal lobe epilepsy. Neuroimage 5:298–306.

Mosher JC, Leahy RM.Recursive MUSIC (1998): A framework for EEG and MEG source localization. IEEE Trans Biomed Eng 45:1342–1354.

Mosher JC, Lewis PS, Leahy RM (1992): Multiple dipole modeling and localization from spatiotemporal Meg data. IEEE Trans Biomed Eng 39:541–557.

Noordmans HJ, van Rijen PC, van Veelen CW, Viergever MA, Hoekema R (2001): Localization of implanted EEG electrodes in a virtual-reality environment. Comput Aided Surg 6:241–258.

Oishi M, Otsubo H, Kameyama S, Morota N, Masuda H, Kitayama M, Tanaka R (2002): Epileptic spikes: Magnetoencephalography versus simultaneous electrocorticography. Epilepsia 43:1390–1395.

Pascual-Marqui RD (2002): Standardized low-resolution brain electromagnetic tomography (sLORETA): Technical details. Methods Find Exp Clin Pharmacol 24:5–12.

Robinson SE, Vrba J, Otsubo H, Ishii R (2002): Finding epileptic loci by nonlinear parametrization of source waveforms. In: Nowak H, Haueisein J, Giessler F, Huonker R, editors. Proceedings of the 13th International Conference on Biomagnetism. VDE Verlag GMBH, Jena, Germany. pp 220–222.

Rosenow F, Luders H (2001): Presurgical evaluation of epilepsy. Brain 124:1683–1700.

Scheler G, Fischer MJ, Genow A, Hummel C, Rampp S, Paulini A, Hopfengärtner R, Kaltenhäuser M, Stefan H (2007): Spatial relationship of source localizations in patients with focal epilepsy: Comparison of MEG and EEG with a three spherical

shells and a boundary element volume conductor model. Hum Brain Mapp 28:315–322.
Sekihara K, Sahani M, Nagarajan SS (2005): Localization bias and spatial resolution of adaptive and non-adaptive spatial filters for MEG source reconstruction. Neuroimage 25:1056–1067.
Shigeto H, Morioka T, Hisada K, Nishio S, Ishibashi H, Kira D, Tobimatsu S, Kato M (2002): Feasibility and limitations of magnetoencephalographic detection of epileptic discharges: Simultaneous recording of magnetic fields and electrocorticography. Neurol Res 24:531–536.
Tao JX, Ray A, Hawes-Ebersole S, Ebersole JS (2005): Intracranial EEG substrates of scalp EEG interictal spikes. Epilepsia 46:669–676.
Tao JX, Baldwin M, Hawes-Ebersole S, Ebersole JS (2007): Cortical substrates of scalp EEG epileptiform discharges. J Clin Neurophysiol 24:96–100.
Trujillo-Barreto NJ, Aubert-Vázquez E, Valdés-Sosa PA (2004): Bayesian model averaging in EEG/MEG imaging. Neuroimage 21:1300–1319.
van 't Ent D, Manshanden I, Ossenblok P, Velis DN, de Munck JC, Verbunt JP, Lopes da Silva FH (2003): Spike cluster analysis in neocortical localization related epilepsy yields clinically significant equivalent source localization results in magnetoencephalogram (MEG). Clin Neurophysiol 114: 1948–1962.
Vrba J, Robinson SE (2001): Signal processing in magnetoencephalography. Methods 25:249–271.
Wagner M, Fuchs M, Kastner J (2004): Evaluation of sLORETA in the presence of noise and multiple sources. Brain Topogr 16:277–280.

## APPENDIX

Details of the following can be found in Mosher et al. [1992] (MUSIC), Pascual-Marqui [2002] and Dalal et al. [2011] (sLORETA), and Vrba and Robinson [2001] (SAM).

## THE FORWARD MODEL

The forward model is defined by:

$$\vec{b}(t) = L\vec{s}(t) + \vec{n}(t) \tag{A1}$$

where $\vec{b}(t)$ is the axial gradiometer data at time $t$ $b_i(t)$ $i = 1, N_g$, $\vec{n}(t)$, $\vec{n}(t)$ is the noise in axial gradiometer at time $t$ $n_i(t)$ $i = 1, N_g$ the number of sensors, $\vec{s}(t)$ is the source strength at time $t$ of unit dipoles $s_j(t)$ $j = 1, N_s$ the number of source points, and $L$ is the lead field matrix $L_{ij}$ $i = 1, N_g$ $j = 1, N_s$.

The source $\vec{s}$ (and corresponding lead field matrix $L$) can be either defined for each of three orthogonal elementary dipoles in Cartesian $\hat{x}, \hat{y}, \hat{z}$ directions (as is the case in the sLORETA implementation) or optimized for a certain dipole orientation $\theta$ as is the case for MUSIC and SAM(g2). $L$ is computed using a single- (MUSIC and sLORETA) or multiple-sphere (SAM) head model. The spatial data covariance matrix $R$ and corresponding noise covariance $N$, both of size $N_g \times N_g$, for a given time interval $T$ are as follows:

$$R = \int_T \vec{b}(t)\vec{b}^t(t)dt \tag{A2}$$

$$N = \int_T \vec{n}(t)\vec{n}^t dt \tag{A3}$$

## MUSIC

In MUSIC, the metric $\mathrm{MUS}_j$ in source points $j = 1, N_s$ is defined as follows:

$$\mathrm{MUS}_j = \frac{1}{\lambda_{\min}(L_j^t E_N E_N^t L_j, L_j^t L_j)} \tag{A4}$$

where $E_N$ is a matrix of eigenvectors $\vec{e}_i$ of $\vec{R}$ $i = r...N_g$ with $1 < r <= N_g$ separating signal from noise subspace and $\lambda_{\min}$ is the minimum generalized eigenvector of the matrix pair parenthesis. $L_j$ (size $N_g \times 3$) is the lead field submatrix for the three elementary dipoles at source location $j$.

## sLORETA

In sLORETA (power of) source strength $\vec{s}(t)$ with $s_j(t)$ $j = 1, N_s$, the number of source points is calculated:

$$\vec{s}(t) = L^t(LL^t + \gamma I)^{-1}\vec{b}(t) \tag{A5}$$

where $I$ is the identity matrix of dimension $N_s \times N_s$ and $\gamma > 0$ a scalar regularization parameter to be chosen allowing inversion of the matrix in parenthesis (Tikhonov regularization). $\vec{s}(t)$ is normalized by its estimated variance $\sigma$ assuming independence of source activity and uniform sensor noise $N = \lambda I$, with prior source variance $\sigma_{\mathrm{prior}} = I$:

$$\sigma = L^t(LL^t + \gamma I)^{-1}L \tag{A6}$$

leading to the sLORETA metric $\mathrm{sLOR}_j$ for source location $j$:

$$\mathrm{sLOR}_j = \vec{s}_j(t)^t \sigma_j^{-1}\vec{s}_j(t) \tag{A7}$$

where the vector $\vec{s}_j$ now refers to the three-dimensional subvector for the elementary dipoles and $\sigma_j$ is the corresponding $3 \times 3$ submatrix.

## SAM(g2)

SAM uses a scalar linearly constrained minimum variance beamformer optimized for unit dipole direction $\theta$:

$$\vec{s}(t) = \frac{L^t R^{-1}}{L^t R^{-1} L}\vec{b}(t) \tag{A8}$$

The SAM(g2) metric computes for $\vec{s}(t)$ the excess kurtosis $\vec{g}_2$ of the amplitude distribution over the time interval $T$ containing $K$ samples:

$$\vec{g}_2 = \frac{\sum_{k=1}^{K}(\vec{s}(t_k) - <\vec{s}>)^4}{K\sigma_{\vec{s}}^4} - 3 \tag{A9}$$

where $<\vec{s}>$ and $\sigma_{\vec{s}}$ are the average and standard deviation of estimated source function amplitude for $K$ samples of each source point $s_j$ $j = 1, N_s$.